https://doi.org/10.5194/egusphere-2025-6498
Preprint. Discussion started: 17 February 2026

A Systemic Shift towards Hydroclimatic Whiplash in India: Event-Based Evidence of Escalating Dry-Wet Transitions since 1951

Debankana Bhattacharjee[1], Chandrika Thulaseedharan Dhanya [2*]

[1] Research Scholar, Department of Civil and Environmental Engineering, Indian Institute of Technology Delhi, New Delhi, India.

[2] Professor, Department of Civil and Environmental Engineering, Indian Institute of Technology, Delhi

***Corresponding author:**

Chandrika Thulaseedharan Dhanya, Professor, Department of Civil and Environmental Engineering, Indian Institute of Technology Delhi, New Delhi-110016, India;

Email: dhanya@civil.iitd.ac.in;

Office Phone Number: +91-11-26597328.

Highlights

- India's hydroclimatic extremes have reorganized fundamentally since the 1980s with extreme wet spells intensifying and expanding by 33 % by 2019, and dry spells shifting southward with marginal frequency changes.
- Rapid dry-to-wet transitions have strengthened by 14.3 %, while spatially expanding by 49 % across tropical coastal and humid subtropical central belts during 1986-2019. However, wet-to-dry transitions declined by 10 % during the later decades along with a decreased spatial footprint, revealing a systematic shift toward convectively driven dry-to-wet whiplash dominance.
- The new risk-based whiplash index reveals a pervasive 13 % rise in extreme risk, and a 26.6% rise in grids experiencing simultaneous high frequency-duration-intensity, indicating a systemic broadening of exposure.
- Chronic high-risk exposure persists over the Southwest coast with no recovery, while emerging risks have triggered a structural 'climate penalty' on agriculture, neutralizing post-2000 technological gains.

Abstract

https://doi.org/10.5194/egusphere-2025-6498
Preprint. Discussion started: 17 February 2026

This study presents a comprehensive assessment of the evolution of hydroclimatic extremes, dry spells (DS), wet spells (WS), and their rapid transitions (whiplash) across India from 1951 till 2019. A marked reorganization of extremes emerged around the 1980s regime shift, characterized by widespread intensification of WS and a 40 % rise in DS-affected grids experiencing fewer but longer events. Using Event Coincidence Analysis, trigger relationships between extreme DS and WS are quantified, revealing that trigger coincidence rates exceeded 0.8 after the mid-1980s and increased spatially by nearly 49 % over the west coast, Central India, and the Northeast. Disaggregating transitions demonstrated an emerging dominance of dry-to-wet (DTW) behavior, with an increase of ~14 %, reflecting reorganized monsoon feedbacks. Quantification of whiplash severity revealed a 13 % and 8.7 % rise in extreme and severe whiplash frequencies, and a 26.6 % increase in grids exhibiting simultaneous high frequency, duration, and intensity. Spatially, the southwest coast and northern India exhibit 'persistently high' risk with no recovery since 1951, while the east coast and central India show 'emerging' volatility. Crucially, this intensification translates into a quantifiable 'climate penalty' on agriculture: post-2000 wheat yields show persistent negative anomalies with an increase in exposure to extreme whiplash risk, which in turn demands an immediate pivot in adaptation and resource planning.

1. Introduction

The rising frequency and intensity of extreme hydro-meteorological events have heightened global concern, particularly as climate change accelerate abrupt transitions between dry and wet extremes, referred here as hydro-meteorological whiplash events, which produce impacts far greater than isolated dry or wet spells (IPCC, 2021; Zscheischler et al., 2018; Vose et al., 2014). Increasingly observed across diverse climatic regimes, these rapid shifts trigger cascading consequences (Weesie et al., 2025; Tan et al., 2023; Zscheischler et al., 2018); for instance, vegetation growth during the preceding wet extremes period can significantly amplify fuel loads, thereby intensifying wildfires in the subsequent dry extreme period (Swain, 2021; Scasta et al., 2016). Furthermore, the surface soil desiccated during dry extremes may develop dense crusts that enhance surface runoff during following wet periods, increasing the likelihood of flooding, landslides (Johnston et al., 2021) and erosion (Borrelli et al., 2020).

Defined not by the duration of the initial state but by the speed and abruptness of transition between opposite hydroclimatic states, whiplash extremes leave minimal time for adaptation and impose severe socio-economic burdens (Anderson et al., 2025; Ansari and Grossi, 2022).

https://doi.org/10.5194/egusphere-2025-6498
Preprint. Discussion started: 17 February 2026

Real-world events, like California's rapid shift from a multi-year drought (2011-2016) to devastating atmospheric-river floods in 2017 causing Oroville Dam failure that displaced 188,000 people (Zhang et al., 2024; Henn et al., 2020; Koskinas et al., 2019; He et al., 2017; Diffenbaugh et al., 2015), or in 2015 South Carolina's transition from a months-long drought to a "1-in-1000-year" flood due to extreme rainfall linked to Hurricane Joaquin (Alipour et al., 2020; Otkin et al., 2015), underscore their compounded, high-impact nature.

This study focuses on the evolution of such whiplash events on India, a region with pronounced monsoon variability which makes it particularly susceptible to such transitions. Over the past six decades, the Indian monsoon has shown an increasing spatial footprint of dry extremes, while wet extremes show no significant trend (Vinnarasi and Dhanya, 2016; Kumar et al., 2020; Singh and Ranade, 2010). High-resolution data analyses reveal intensifying rainfall heterogeneity, with wet regions turning drier and vice versa (Singh et al., 2021;Katzenberger et al., 2020; Vinnarasi and Dhanya, 2016). Extreme precipitation events are strongly modulated by large-scale climate modes, such as the Indian Summer Monsoon Index and Arctic Oscillation (Rehana et al., 2022; Kumar et al., 2020; Singh and Ranade, 2010), which modulate atmospheric circulation and monsoon strength.

While earlier studies have examined transitions between wet and dry regimes on seasonal or annual scales (Madakumbura et al., 2021; Casson et al., 2019; Christian et al., 2015), high-resolution analyses capturing daily resolved and sub-seasonal whiplash dynamics remain underexplored, especially over monsoon-dominated regions. To examine the switch between long-term dry and wet regimes, anomalous annual precipitation dipole events (a dry year followed by a wet year (Christian et al., 2015)) and seasonal precipitation anomalies (a dry winter one year followed by a wet winter the next) have been analyzed (Swain et al., 2018). However, such coarse temporal aggregations cannot capture the rapid transitions that constitute a whiplash, occurring within months or weeks, over India (Dash and Maity, 2021).

Despite substantial progress in characterising dry, wet, and compound extremes using: (i) univariate standardized indices (like, Standardized Precipitation Index (SPI) (Guttman, 1998), Standardized Precipitation and Evapotranspiration Index (SPEI) (Vicente-Serrano et al., 2010)) that aggregate precipitation (and sometimes evapotranspiration) over fixed accumulation windows to quantify wetness/ dryness relative to a historical climatology (Laimighofer and Laaha, 2022; He and Sheffield, 2020); (ii) multivariate and joint probability approaches (multivariate extreme value theory, copulas, joint return periods) that estimate co-occurrence probabilities of extreme magnitudes (Zscheischler and Seneviratne, 2017; Salvadori et al., 2007; Coles et al., 2001); and (iii) process-based or model-based analyses that use coupled

https://doi.org/10.5194/egusphere-2025-6498
Preprint. Discussion started: 17 February 2026

land-atmosphere models to diagnose feedbacks and drivers (Miralles et al., 2019; Seneviratne et al., 2010), a critical knowledge gap remains in detecting and quantifying short-lag, directional transitions between hydroclimatic states. Existing approaches rely on fixed accumulation windows, stationary assumptions (Laimighofer and Laaha, 2022; IPCC, 2021;He and Sheffield, 2020), or magnitude-based dependence structures that smooth intra-seasonal variability and fail to capture the sequencing, timing, or rapid onset of transitions (Miralles et al., 2019; Salvadori et al., 2007; Coles et al., 2001), limitations that are particularly consequential for the highly variable and rapidly shifting Indian monsoon system (Mishra et al., 2024; Tan et al., 2023; Bhattacharyya et al., 2022; Krishna et al., 2020). Consequently, the spatiotemporal evolution of the interaction between dry and wet spells, and the mechanisms by which they produce high-impact whiplash events, remain poorly resolved. To address this gap, this study employs a daily, event-based, non-parametric framework (Donges et al., 2016; Siegmund et al., 2017; Walters, 2012) that uses raw precipitation, the most direct hydrometeorological driver (Pendergrass et al., 2017; Trenberth et al., 2003), to identify individual extremes and their rapid transitions without imposing parametric, stationary, or aggregation constraints. This study enables explicit detection of short-lag directional links between precursor dry or wet events and their subsequent triggers, allowing a robust, observation-driven reconstruction of how whiplash dynamics have reorganized across India's climatic zones over the past seven decades (1951-2019).

Therefore, the overall objectives of this study are: (i) to detect and characterize short-lag hydroclimatic whiplash transitions, including their directionality, strength, and lag structure, using an event-based, non-parametric framework, (ii) to identify emerging regional hotspots and climate-zone specific behaviors in the whiplash occur occurrences under evolving monsoon variability, and (iii) to capture concurrent changes in frequency, duration, and intensity of rapid spell transitions, using an integrated whiplash risk index.

This article is organized as follows: Section 2 details the dataset and the study area. Section 3 describes the methodology, which is followed by the Results and Discussions in Section 4, and the conclusions in Section 5.

2. Study Area and Data Used

This study focuses on the Indian subcontinent spanning over 3.29 million km^2, a densely populated and agriculturally reliant country. The Indian subcontinent encompasses highly diverse climate zones (figure 1) (Beck et al., 2018; Peel et al., 2007; Köppen, 1884), including

https://doi.org/10.5194/egusphere-2025-6498
Preprint. Discussion started: 17 February 2026

arid and semi-arid regions in the northwest, warm temperate zones in central India, subtropical humid areas in the northeast and Himalayan foothills, semi-arid and tropical wet-and-dry regions in the south, and warm-humid coastal belts. This climatic heterogeneity makes India vulnerable to both hydro-meteorological extreme wet and dry spells. This study utilizes a high-resolution daily gridded precipitation dataset (0.25 °× 0.25 °) (Pai et al., 2014), obtained from the India Meteorological Department (IMD) for the period of 1951-2019. The dataset spans the spatial domain from 6 ° to 38 °N latitude and 68 ° to 100 °E longitude.

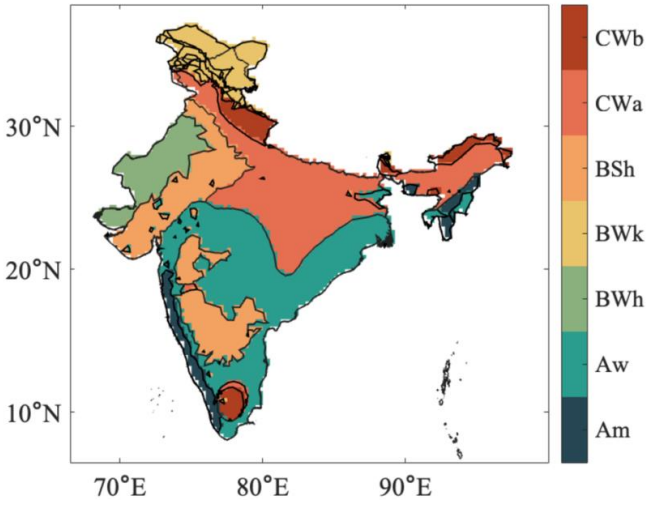

Figure 1: Details of climatic zones and their spatial extent over India (Tropical Monsoon/Tropical Wet [Am], Humid Subtropical/Temporal [Cwa], Hot Desert/Arid [BWh], Hot Semiarid/Arid Steppe and Hot [BSh], Tropical Wet and Dry/Tropical Savannah [Aw], and Warm Temperate [Cwb]).

3. Methodology

3.1. Identification of individual dry and wet spells

In this study, extreme events are defined and extracted from daily precipitation at each grid point of India over 1951-2019. An extreme dry spell (DS) is defined as a period where the daily precipitation remains below the 5th percentile continuously for at least a month, indicating a prolonged deficit in rainfall. This threshold is consistent with widely accepted definitions of short-term meteorological dry extremes (Vicente-Serrano et al., 2010; Wilhite and Glantz, 1985) and has been employed in previous studies over India to capture prolonged hydro-

https://doi.org/10.5194/egusphere-2025-6498
Preprint. Discussion started: 17 February 2026

meteorological stress with significant impacts on agriculture, water resources, and ecosystems (Tandel et al., 2023; Dash and Maity, 2021; Vinnarasi and Dhanya, 2016).

In contrast, an extreme wet spell (WS) is identified as a day or sequence of days exceeding the 95th percentile of daily precipitation, signifying a sudden and intense rainfall event (Dash and Maity, 2021; Swain et al., 2018; Vinnarasi and Dhanya, 2016). The choice of the 5th and 95th percentiles ensures a focus on the most extreme tails of the precipitation distribution, capturing events with the greatest potential hydrological and socio-economic impacts (Swain et al., 2018; Pendergrass et al., 2017).

Extended dry phases lasting several weeks can substantially deplete soil moisture, reduce groundwater recharge, and suppress vegetation growth, while isolated but intense wet events can trigger flash floods, landslides, and rapid erosion (Johnston, 2024; Pal and Ojha, 2021; Borelli et al., 2020). While intermittent dry days are a natural part of the monsoon cycle, a DS of ≥ 30 consecutive days below the 5th percentile within the monsoon season represents an anomalous break phase rather than a typical intra-seasonal fluctuation, severely impacting rainfed agriculture and water resources even during the monsoon months (Straus, 2022; Kumar et al., 2013). Similarly, extreme WS exceeding the 95th percentile often corresponds to high-impact flood-producing events associated with active monsoon phases (Goswami et al., 2006).

3.2. Detection of localized spatial clusters of extreme frequency shifts

To further investigate spatial coherence in the frequency shifts of extreme DS and WS, the Getis Ord G_i^* statistic (Getis and Ord, 1992) is employed. This spatial statistic quantifies the degree to which high or low values of a variable cluster in geographic space, distinguishing statistically significant local "hot" and "cold" regions. The G_i^* statistic for each grid cell i is computed as:

$$G_i^* = \frac{\sum_j w_{ij} x_j - \bar{X} \sum_j w_{ij}}{S \sqrt{\frac{\left[n \sum_j w_{ij}^2 - \left(\sum_j w_{ij}\right)^2\right]}{n-1}}} \quad (1)$$

where x_j is the attribute value (here, standardized frequency change in DS or WS) at location j, w_{ij} is the spatial weight between locations i and j, n is the total number of observations, $\bar{X}$ is the mean, and S is the standard deviation of all x. The resulting z-scores quantify how strongly each grid cell is associated with spatially clustered high or low values, while corresponding p-values indicate statistical significance.

https://doi.org/10.5194/egusphere-2025-6498
Preprint. Discussion started: 17 February 2026

In this study, grids with significant positive G_i^* values ($z > 1.96$, $p < 0.05$) were identified as hotspots, representing clusters of high-frequency changes in DS or WS, whereas significant negative G_i^* values ($z < -1.96$, $p < 0.05$) were defined as coldspots, indicating localized decreases. The spatial weights (w_{ij}) were defined using a fixed-distance neighborhood matrix to capture immediate local interactions while minimizing edge effects. By mapping only statistically significant clusters, the G_i^* analysis provides a robust visualization of regional redistribution and intensification patterns of DS and WS frequencies over time. This enables the detection of spatially coherent zones of increasing or declining individual extremes, offering valuable insights into evolving hydroclimatic risk landscapes across diverse climate zones of India. However, understanding their temporal interplay is critical for capturing rapid phase transitions between these opposing extremes, to finally identify potential whiplash occurrences and elucidating the dynamics governing those transitions across India.

3.3.Event Coincidence Analysis (ECA)

We adopt an event-based, non-parametric framework, Event Coincidence Analysis, which as the name implies, quantifies how often two types of events occur in close temporal succession (Donges et al., 2016, 2015; Siegmund et al., 2017), to explicitly quantify the coincidence rate and lag structure (both instantaneous and lagged response) between the two temporary successive events. Here, ECA is used to evaluate the bidirectional temporal relationship between extreme dry and wet spells, i.e., how often a DS is followed by a WS within a specified short lag window and vice versa. Furthermore, ECA does not require aggregation into long accumulation windows, while preserving sequencing and directionality (Walters, 2012). The timing of the clearly defined events is the only factor considered by ECA. As a result, it facilitates the assessment of the statistical relationship and temporal co-occurrence among the phenomena and/or processes being examined (Donges et al., 2016, 2015; Siegmund et al., 2017).

ECA also serves as a tool for testing hypotheses about the nature of the connections between two event types, such as whether one acts as a precursor (causal trigger), a consequence, or a co-occurring phenomenon under shared climatic drivers (Donges et al., 2016, 2015; Siegmund et al., 2017). For example, in hydroclimatic contexts, a dry-to-wet transition might reflect atmospheric circulation shifts or large-scale moisture advection processes, whereas a wet-to-dry transition might be linked to post-storm soil moisture feedbacks or suppressed convection following heavy rainfall. Thus, ECA facilitates the exploration of physical mechanisms

https://doi.org/10.5194/egusphere-2025-6498
Preprint. Discussion started: 17 February 2026

underlying the temporal sequencing of extremes, which cannot be inferred from linear correlation analyses alone.

To determine the degree of statistical correlation between the two-event series, ECA offers two coincidence metrics, namely the precursor and trigger coincidence rates.

3.3.1. Precursor Coincidence Rate

The Precursor Coincidence Rate quantifies the likelihood that an extreme event (e.g., a DS) acts as a precursor to a subsequent extreme (e.g., a WS) within a defined time window, thereby serving as a diagnostic measure of dry-to-wet whiplash transitions. In the context of hydro-meteorological extremes, a high precursor rate indicates a strong temporal clustering of opposite-phase events, suggesting that antecedent dry conditions may enhance the susceptibility of the system to rapid wet transitions due to reduced infiltration, soil crusting, or hydrological memory effects. Conversely, a low rate implies that the two extremes are largely independent with minimal temporal coupling.

Mathematically, consider the time series of WS and DS occurring, respectively, at times t_i^{WS} and t_j^{DS} with $i = 1, \ldots, N_{WS}$ and $j = 1, \ldots, N_{DS}$, where N_{WS} and N_{DS} are the number of WS and DS events, respectively. The precursor coincidence rate (r_p) is defined as (Donges et al., 2016, 2011) (also shown in figure 2):

$$r_p = \frac{1}{N_{WS}} \sum_{i=1}^{N_{WS}} H\left(\sum_{j=1}^{N_{DS}} I_{[0,\Delta T]}\left(\left(t_i^{WS} - \tau\right) - t_j^{DS} \right) \right) \quad (2)$$

Here τ is the lag parameter between the two events types and controls the admissible recovery time between a potential precursor and a subsequent opposite-phase extreme. ΔT is defined as the temporal tolerance for preconditioning with a time window of a specific period from τ. $I_{[0,\Delta T]}(x)$ is an indicator function which equals 1 if the event $\left(\left(t_i^{WS} - \tau\right) - t_j^{DS}\right)$ lies within the window ΔT, and 0 otherwise, and $H\ (x)$ denotes the Heaviside function. For WS occurring at time t_i^{WS}, the output of the Heaviside function is either one or zero based on the following rule:

$$H\left(\sum_{j=1}^{N_{DS}} I_{[0,\Delta T]}\left(\left(t_i^{WS} - \tau\right) - t_j^{DS} \right) \right) = \begin{cases} 1, & \left(\sum_{j=1}^{N_{DS}} I_{[0,\Delta T]}\left(\left(t_i^{WS} - \tau\right) - t_j^{DS} \right) \right) > 0 \\ 0, else & \end{cases} \quad (3)$$

which indicates whether or not the WS- event under consideration has a preconditioning impact. The remaining WS-events are then subjected to the same procedure. Lastly the

https://doi.org/10.5194/egusphere-2025-6498
Preprint. Discussion started: 17 February 2026

Precursor Coincidence Rate r_p calculates the fraction of WS events preceded by DS occurrences, with values ranging from 0 (which indicates no preconditioning) to 1 (indicating all WS events are preconditioned by DS).

3.3.2. Trigger Coincidence Rates

Another measure of the statistical link between the two series under investigation which ECA employs is the trigger coincidence rate. Complementary to the Precursor Coincidence Rate, the Trigger Coincidence Rate quantifies how frequently an extreme event (e.g., a WS) is followed by an opposite extreme (e.g., a DS) within a defined time window. In the context of hydroclimatic whiplash, a high trigger rate indicates that intense wet conditions are often succeeded by rapid drying, implying strong post-event land-atmosphere feedbacks such as enhanced evapotranspiration, rapid soil moisture depletion, or suppressed subsequent rainfall due to convective stabilization. Conversely, a low trigger rate suggests that wet extremes occurred largely in isolation without immediate dry transitions.

Mathematically, consider the time series of WS and DS occurring, respectively, at times t_i^{WS} and t_j^{DS} with $i = 1, \ldots, N_{WS}$ and $j = 1, \ldots, N_{DS}$, where N_{WS} and N_{DS} are the number of WS and DS events, respectively. The trigger coincidence rate (r_t), when focused on DS, is defined by (Donges et al. 2016, 2011) as (also shown in figure 2):

$$r_t = \frac{1}{N_{DS}} \sum_{i=1}^{N_{DS}} H\left(\sum_{j=1}^{N_{WS}} I_{[0,\Delta T]}\left(\left(t_i^{WS} - \tau\right) - t_j^{DS} \right) \right) \quad (4)$$

Here, the Heaviside function $H(x)$ captures whether a DS event triggers a WS event within the lag tolerance. Conversely, if the analysis focuses on WS triggers, it measures whether a WS is followed by a DS. This procedure is repeated for all events of the designated trigger type, yielding r_t values in the range of 0 (no triggering) to 1(every trigger event is followed by a response event).

https://doi.org/10.5194/egusphere-2025-6498
Preprint. Discussion started: 17 February 2026

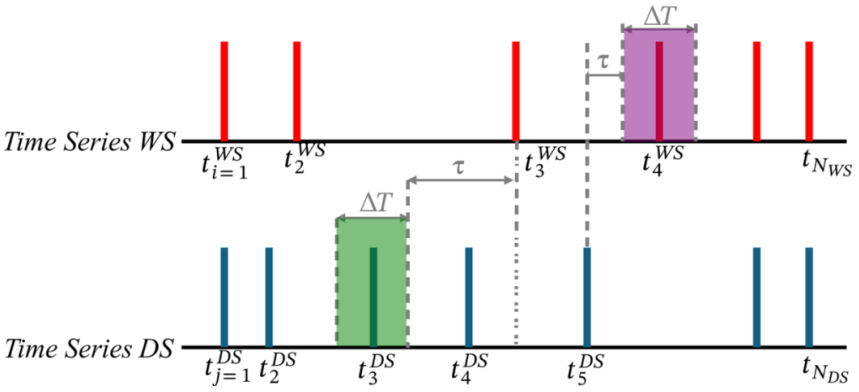

Figure 2: Schematic illustration of Precursor and Trigger Coincidence Rates; To calculate PCR, the WS (red bars) at t_3^{WS} is considered, precursor coincidence occurs when a DS (blue bars, here t_3^{DS}) falls within the prefixed temporal tolerance window ΔT (green box), at a lag of τ from t_3^{WS}, which is then repeated for all WS, and the total number of coincidences is calculated. To calculate TCR, the DS (blue bar) at t_5^{DS} is considered, trigger coincidence occurs when a WS (red bars, here t_4^{WS}) falls within the prefixed temporal tolerance window (purple box), at a lag τ from t_5^{DS}, Which is then repeated for all DS, and the total number of trigger coincidences are calculated.

4. Results and discussions

4.1. Spatiotemporal variation of individual DS and WS around the 1980s regime shift

A distinct decline in WS frequency trends is evident until the 1980s, followed by a marked increase thereafter (See the Supplementary Material, figure S1 that identifies the shift through the decadal redistribution of extreme DS and WS). Although DS frequencies remained comparatively stable across decades, their spatial footprint evolved considerably. The period 1981-1990 thus represents a transition phase, warranting the segregation of pre- and post-1980s epochs to highlight the redistribution and intensification of extremes in changing climate.

Further analysis of the climatological evolution of extreme DS revealed a notable spatial spread and redistribution between the two time periods: 1951-1985 and 1986-2019 as shown in Figure 3(a-i). Although a reduction in DS frequency was observed over northwestern (BWh) and central India (CWa) during the later period, the spatial spread extended southward. When statistically significant clusters were retained using the Getis-Ord G_i^* Statistic and mapped for further interpretation (figure 3(a-ii)), it revealed that western Rajasthan (BWh) exhibited increased DS frequency, along with Uttarakhand (Cwb/ Aw), northern UP (Cwa), parts of

https://doi.org/10.5194/egusphere-2025-6498
Preprint. Discussion started: 17 February 2026

Jharkhand (Aw) and southern West Bengal (Cwa), and parts of Maharashtra, Telangana, Andhra Pradesh, and Chhattisgarh, spanning Am and Aw climate zones.

Conversely, extreme WS showed a broad-scale intensification and spatial expansion between 1986-2019 compared to 1951-1985 (figure 3(b- i)). Statistically significant WS hotspots emerged in arid Rajasthan, coastal Karnataka and Kerala (Am), extending to semi-arid Maharashtra and certain pockets of the northeastern states (Am) (figure 3(b- ii)). Such growing exposure of both arid and humid climatic regions to high-frequency extreme WS, reflects a spatial reorganization of hydroclimatic stress across diverse climate regimes. Overall, the distributional shifts in affected grids (figure 3(c)) indicates an increase of up to 40 % in the area experiencing 2-4 DS per year and an increase of up to 33-50 % in the areas undergoing 12 or more WS per year during 1986-2019.

The observed spatial and temporal shifts in both DS and WS indicate a growing spatial overlap and temporal proximity between opposing hydroclimatic states, thereby increasing the likelihood of rapid transitions between them. Regions that were once dominated by prolonged dry conditions may now experience intensified wet extremes. Such oscillations, termed here as hydroclimatic whiplash, cannot be fully captured by examining DS and WS independently. A focused investigation of these transition dynamics using Event Coincidence Analysis (ECA) therefore provides crucial insight into the evolving compound nature of India's monsoon extremes.

https://doi.org/10.5194/egusphere-2025-6498
Preprint. Discussion started: 17 February 2026

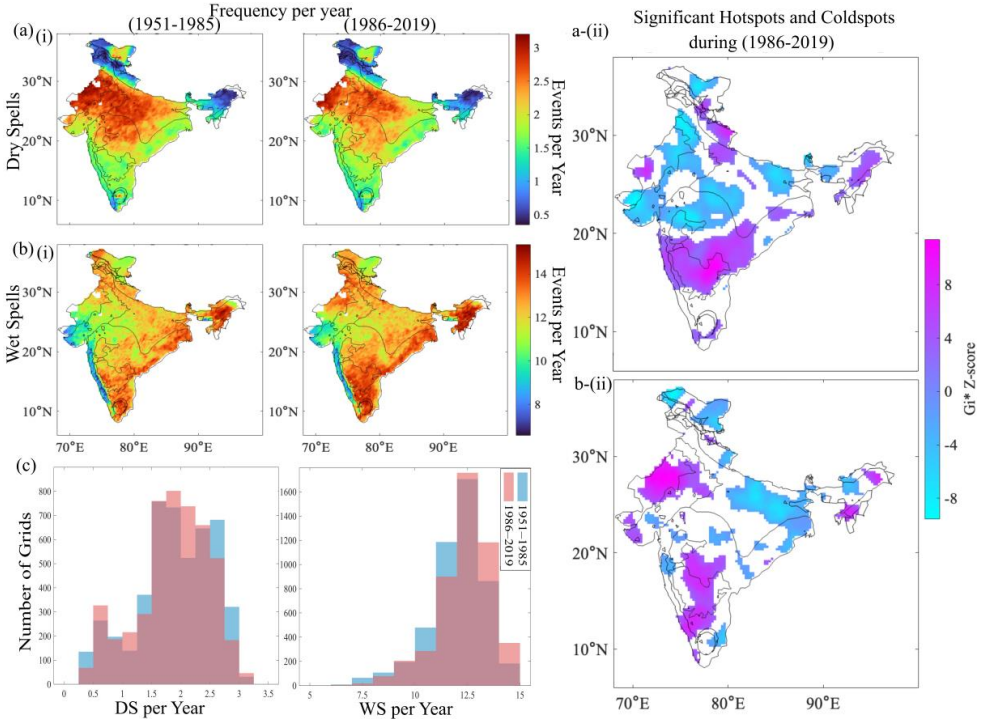

Figure 3: (a) (i) Spatial distribution of average annual frequency of extreme Dry Spells (DS) during 1951-1985 and 1986- 2019; (ii) Significant hotspots and coldspots identified for the DS frequency change during 1986- 2019 using the Getis-Ord G_i^* score; (b) (i) Spatial distribution of average annual frequency of extreme Wet Spells (WS) during 1951-1985 and 1986- 2019; (ii) Significant hotspots and coldspots identified for the WS frequency change during 1986- 2019 using the Getis-Ord G_i^* score; (c) Distribution of the number of grids experiencing different frequencies of extreme DS and WS during 1951-1985 (blue) and 1986- 2019 (red).

4.2.Evolving dynamics and directional asymmetry in India's whiplash behavior

The climatology of whiplash events is analyzed using ECA to assess the compound behavior of extreme WS and DS across India distinguishing between trigger and precursor relationships. The resulting frequency and spatial patterns illuminate emerging shifts in the country's extreme-event dynamics.

Figure 4(a) illustrates high ($r_t > 0.7$) trigger coincidence rates during 1951-1985 and its spatial concentration over the entire western coastal belt (Am), the Northeastern states (Am), and parts of Eastern and Central India (Aw/ Cwa). During 1986-2019, not only did these regions retain

https://doi.org/10.5194/egusphere-2025-6498
Preprint. Discussion started: 17 February 2026

high coincidence rates, but the magnitudes intensified ($r_t > 0.8$) and expanded spatially. Clearly, this establishes the intensification of whiplash transitions and its spread over climatically sensitive zones in recent decades. The precursor coincidence rates (figure 4(b)) showed very high values which were mainly prominent over Western Ghats (Am) and North Bengal (Cwa) during 1951-1985, suggesting a strong preconditioning mechanism where the prior extreme sets the stage for a subsequent one. While the magnitude remained similar over those regions during 1986-2019, Eastern India (Cwa) marked an increase of 33.3 % in average precursor rates along with an increased spread over the Northeast (Am). This enhanced precursor coupling is indicative of a persistence-driven mechanism or a hydroclimatic memory effect, particularly over the east and Northeast regions (Cwa/ Am), wherein antecedent soil moisture deficits or excesses modulate the land atmosphere feedbacks that predispose regions to rapid transitions between extremes, as reported in earlier studies (Götte and Brunner, 2021; Koster et al., 2010)

The spatial distribution of coincidence values is further summarized in figure 4(c). The increase in the number of grids exhibiting trigger rates between 0.5 and 1 during 1986-2019 further reinforces the intensifying and spreading nature of whiplash behavior. In contrast, precursor coincidence rates remained constrained to less than 500 grids in both periods, despite increased intensity in select regions. This implies that while triggering relationships have become more widespread, precursor relationships remain more localized, likely due to region specific land surface feedbacks.

Further, the sensitivity of the ECA metrics to key analytical parameters (lag time (τ) and time window (ΔT)) was investigated (figure 4(d)). When the lag was increased from 1 month to 3 months (ΔT = 1 year), both trigger and precursor coincidence rates decreased significantly by 34.5 % and 21.3 %, respectively. This emphasizes that most whiplash transitions occur within a short lag window, highlighting the rapid onset nature of these events, which poses severe challenges for early warning systems and disaster preparedness. Conversely, increasing the time window from 1 year to 5 years (τ = 3 months) led to an increase of over 50 % in both rates, indicating that when a broader temporal lens is used, more extreme spell transitions are captured. This suggests that multi-annual persistence or recovery effects might also contribute to longer- term whiplash behavior. These findings are further substantiated by Figure S2(a) for trigger and Figure S2(b) for precursor rates (Supplementary material), where a clear decline in both intensity and spatial spread is observed with increasing lag, while the opposite is true for larger time windows.

https://doi.org/10.5194/egusphere-2025-6498
Preprint. Discussion started: 17 February 2026

Given the dominance of trigger behavior, further disaggregation into DS Triggering WS (DTW) and WS Triggering DS (WTD) was conducted (figure 4(e)). This analysis reveals an interesting asymmetry. DTW rates ranging 0.3-0.6 (showing moderate temporal variability), increased by ~4 % in 1986-2019 relative to the earlier period, whereas WTD rates, though higher in magnitude (0.7-0.8) and much lower temporal variability, decreased by ~10 %. Although the overall differences are modest, their opposing directions indicate a gradual shift in dominance from wet-to-dry towards dry-to-wet transitions. Figure 4(f) and the spatial maps shown in Figure S2(c) (Supplementary Material), support these trends: DTW shows a prominent spatial footprint, while WTD, though more frequent, shrinks in spread. This contrast likely reflects a reorganization of hydroclimatic feedback that enhances DTW occurrences, resulting under evolving monsoon dynamics, where intensified convector activity following prolonged dry conditions, driven by land-surface heating and boundary layer destabilization (Liu et al., 2022; Zhou and Geerts, 2013). Whereas weakening post-monsoon subsidence and reduced soil moisture-precipitation coupling may limit WTD events (Seneviratne et al., 2010; Dirmeyer et al., 2009). Anthropogenic warming and aerosol-induced monsoon modulation further alter large-scale circulation, reducing wet phase persistence and reshaping event sequencing (Ayantika et al., 2021), thereby collectively driving a shift toward more convectively driven DTW transitions and fewer WTD reversals.

To further compare the evolving nature of the individual hydroclimatic extremes, and their whiplash behavior in the recent decades, we analyzed the frequency ratio of DS, WS and their whiplash (trigger rates), comparing the recent period (1986-2019) to the earlier baseline (1951-1985) (figure 4(g)). While DS have increased marginally across most regions (0.7 %), WS show more pronounced and spatially widespread rise (4-5 %) especially over western (BWh), central (Aw), and eastern India (Cwa), signaling an intensification of extreme wet periods. However, it is the whiplash behavior which stands out. Though spatially limited, the frequency of whiplash has increased across the west coast (Am), with a sharp increase (almost 49 %) along the central belt (Aw) and Northeast (Am). This highlights the growing propensity of rapid whiplash occurrences. These regions are not just facing more extremes, but more abrupt switches between dry and wet conditions, which in turn indicates a shift towards volatile monsoon dynamics.

https://doi.org/10.5194/egusphere-2025-6498
Preprint. Discussion started: 17 February 2026

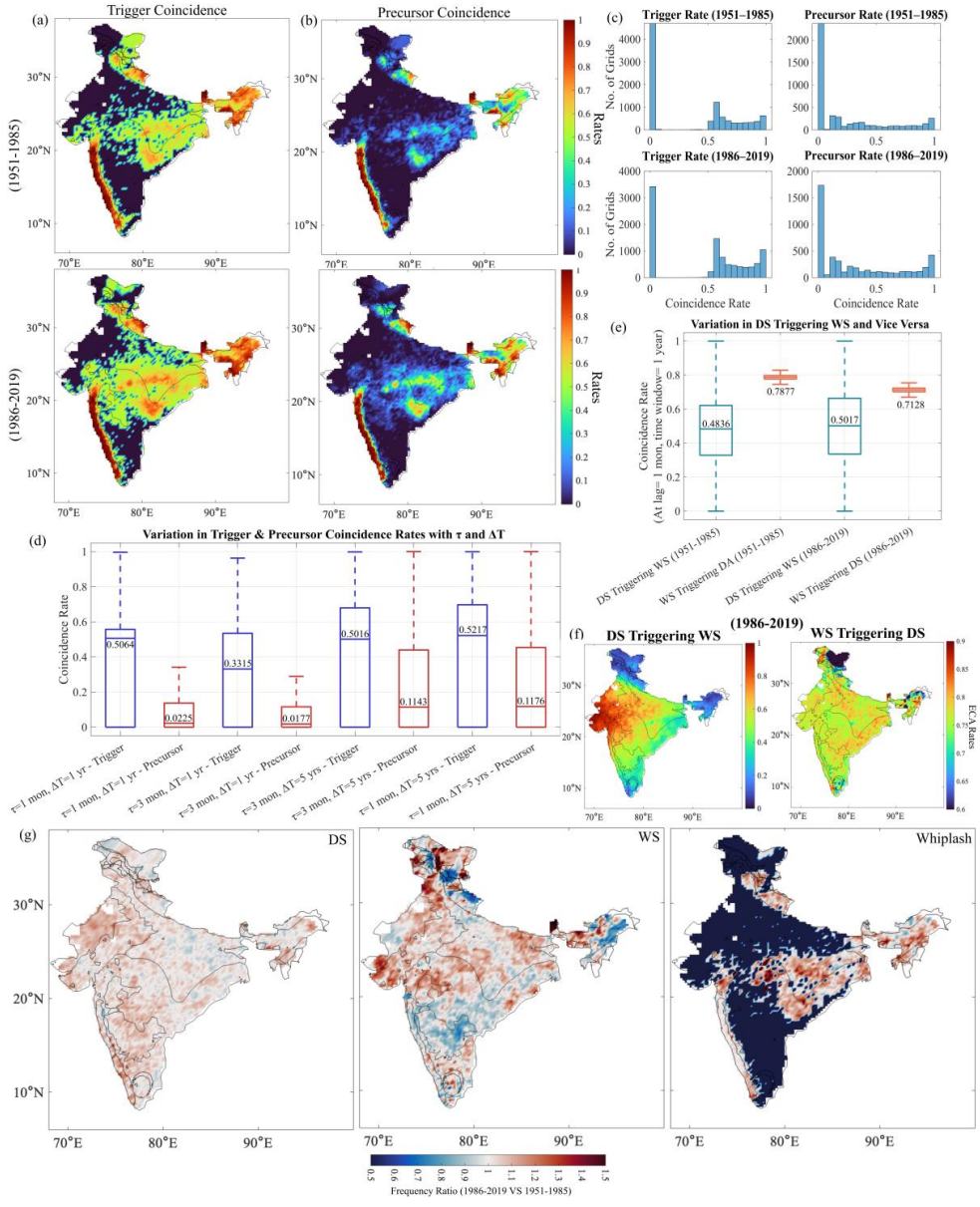

Figure 4: (a) Spatial distribution of trigger coincidence rates over India during the two time periods: 1951-1985 and 1986-2019; (b) Spatial distribution of precursor coincidence rates over India during the two time periods: 1951-1985 and 1986-2019; (c) Grid-wise distribution of precursor and trigger rates during 1951-1985 and 1986-2019 across India, shows lower distribution for precursor and higher for trigger; (d) Sensitivity of trigger and precursor coincidence rates to lag (τ) and time window (□T), the two parameters

https://doi.org/10.5194/egusphere-2025-6498
Preprint. Discussion started: 17 February 2026

used in the Event Coincidence Analysis; (e) Comparison of DS Triggering WS (DTW) and WS Triggering DS (WTD) coincidence rates across the two time periods; (f) Spatial maps of DTW and WTD coincidence rates for the period 1986-2019; (g) Frequency ratio of the DS, WS and their whiplash behaviour over the last 35 years (1986-2019) and the first 35 years (1951-1985).

4.3. Non-linear sensitivities and emerging whiplash risk typologies

To systematically understand the spectrum of hydroclimatic whiplash events across India, we categorized compound extremes by combining the variations in DS and WS characteristics. Specifically dry extremes were defined across three durations of 1 month, 6 months, 12 months, and three intensity thresholds of 15th percentile, 10th percentile, and 5th percentile. Similarly wet extremes were characterized by durations of 1 day, 5 days, and 10 days, and intensities exceeding the 85th, 90th and 95th percentiles. This multidimensional combination led to the creation of 81 distinct whiplash categories, some including 1-month DS of < 5th percentile (Dry1mon5p) followed by WS of 1 day of > 95th percentile (W1d95p), 6 months DS of < 10th percentile (Dry6mon10p) followed by WS of 5 days > 85th percentile (W5d85p), and so on. To focus on the intrinsic variability of these compound categories, a single representative lag period of one month was applied uniformly across all combinations.

Figure 5(a) presents the frequency of these 81 categories over the recent hydroclimatic epoch 1986-2019, revealing several notable trends. Peak frequency was observed for the whiplash of 6-months DS of < 15th percentile (Dry6mon15p) and 1-day WS of > 95th percentile (W1d95p), highlighting the increasing prominence of rapid wet recoveries following prolonged moderate dry periods. While increasing the DS duration from 1 month to 6 months whiplash occurrences increased by ~73 %, but further extension to 12 months led to a marked decrease. This non-linear sensitivity arises because intermediate-duration DS are sufficiently frequent and induce strong land-atmosphere coupling, making them highly conducive to abrupt WS transitions. In contrast, very short DS lack the persistence required to generate a rapid wet rebound, while year-long DS are too rare and governed by slower hydroclimatic recovery processes to produce frequent whiplash pairing. Consequently, whiplash likelihood peaks at moderate DS durations. On the other hand, increase in WS duration from 1 day to 10 days generally decreased the whiplash frequency, and decrease in WS intensity thresholds from 95th to 85th percentile, increased the frequency. This indicates that short intense wet events are the key triggers. Further, a comparison with the baseline epoch (1951-1985) (Figure S3 in Supplementary

https://doi.org/10.5194/egusphere-2025-6498
Preprint. Discussion started: 17 February 2026

material) reveals a modest but consistent increase (7.2 %) in ECA frequencies across all categories, implying a widespread intensification of whiplash sequences over time.

To further distil actionable insights from the 81-category space, three representative cases were selected (figure 5(b)), grounded in extreme event theory and impact relevance: (i) Best Case (BC): 1 month DS of < 15th percentile (Dry1mon15p) followed by 10 days WS of > 85th percentile (W10d85p), representing benign, hydrologically balanced recovery which is a desirable resilient scenario; (ii) Worst Case (WC): 365 days DS of < 5th percentile (Dry12mon5p) followed by a flash WS of 1 day and > 95th percentile (W1d95p), reflecting a highly stressful scenario, posing threats to both ecosystem and infrastructure; (iii) Flash Case (FC): DS of 1 month and < 5th percentile (Dry1mon5p) followed by WS of 1 day of > 95th percentile (W1d95p), emphasizing a sudden onset, short duration shocks with high intensity, likely a growing concern under climate variability. The BC moderate frequency increased by 25% in 1986-2019 hinting at slight improvements in some regions' DS-WS recoveries. However, the WC remained alarmingly high, ranging from 55 % to 57 %, and so is the FC, ranging from 56 % to 59 %, reinforcing the dominance of stress- inducing events in shaping hydroclimatic risk landscapes. These trends point to worsening whiplash, especially dominated by rapid onset extremes, even though isolated "best-case" recoveries exist in pockets.

Figure 5(c) further reveals distinct regional patterns of the spatial footprint of the three representative cases. BS and FC were largely concentrated in the western parts of the Western Ghats (Am), Northeast India (Am), and Eastern India (Cwa), regions known for strong monsoonal signatures and steep terrain. WC, by contrast, was primarily focused on Western and Northwestern India, coinciding with the arid and semi-arid zones vulnerable to persistent DS and sudden WS. During 1986-2019, while the spatial extent of BC and FC expanded into Central (Aw) and parts of Western India (BSh), WC regions showed further intensification rather than spread, representing chronic compound risk in already vulnerable regions. This spatial divergence, where some regions see expansion of flash or benign scenarios while others exhibit intensification of chronic stress, is critical for informing region-specific adaptation strategies.

https://doi.org/10.5194/egusphere-2025-6498
Preprint. Discussion started: 17 February 2026

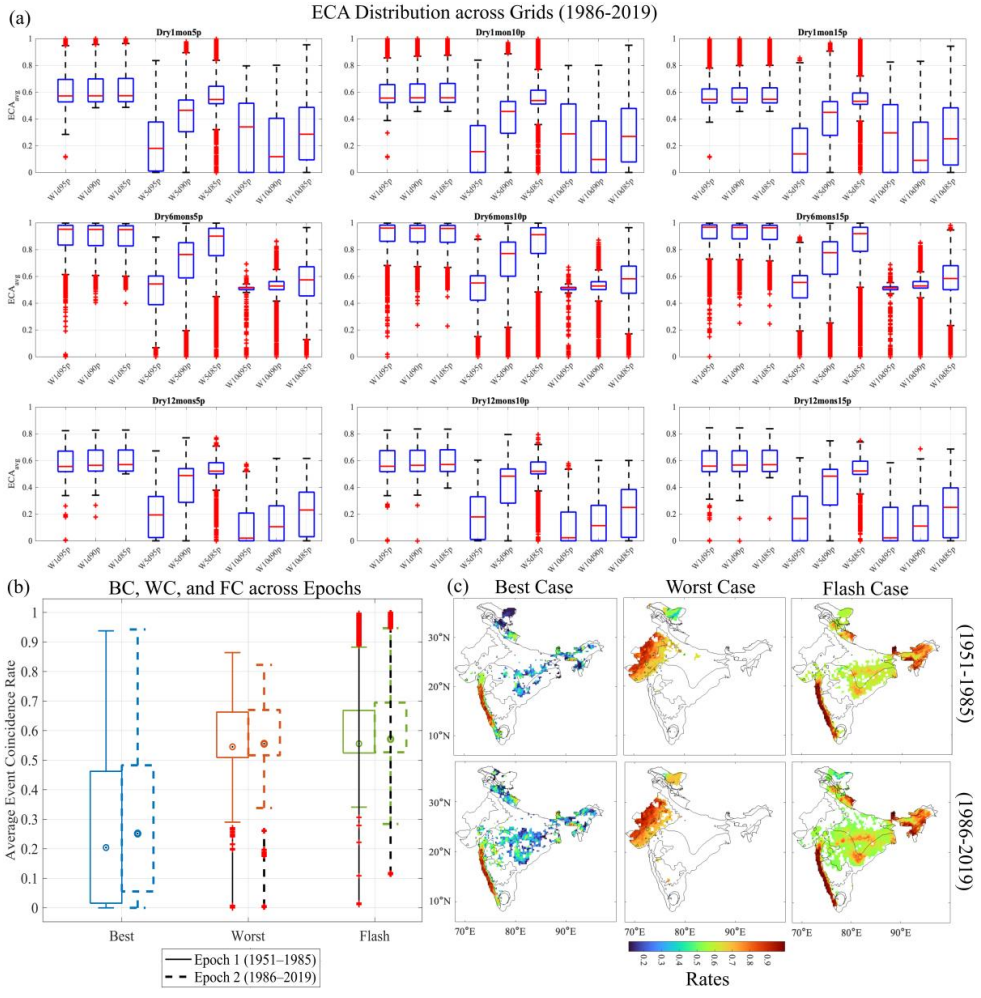

Figure 5: (a) Frequency distribution of 81 compound DS-WS categories during 1986-2019, constructed by varying the duration and intensity of individual DS and WS; (b) Comparison of three representative compound cases- Best Case (BC), Worst Case (WC), and Flash Case (FC)- highlighting their frequency changes between 1951-1985 and 1986-2019; (c) Spatial extent of the Best, Worst, and Flash Cases across India for the two epochs.

4.4.Quantifying whiplash severity using a lag-weighted whiplash risk index (CEI)

Although till now the whiplash transitions were quantified through isolated case analysis, a quantitative and temporally consistent index could more effectively capture the characteristics of the whiplash events. Therefore, a Compound Event Index (CEI) is proposed while focusing

https://doi.org/10.5194/egusphere-2025-6498
Preprint. Discussion started: 17 February 2026

on the most impactful and climatically significant type of whiplash transition identified across India in section 4.2., i.e., DTW. The CEI is computed by aggregating the frequencies of DTW transitions across lag windows (l) from 1 month to 9 months (Eq. 5).

$$CEI = \sum_{l=1}^{9} \left(DTW_l \middle| Weight(l) \right) \quad (5)$$

These lags represent the typical range over which terrestrial and atmospheric systems attempt to recover from prolonged extreme conditions. Section 4.2. also revealed that the frequencies decreased with increasing lag, indicating that short-lag transitions are more common and potentially more abrupt. Therefore, weights $\left(Weight(l)\right)$ are assigned inversely proportional to the lag duration, to ensure that shorter-lag transitions are given more importance, reflecting their limited recovery windows and higher likelihood of inducing stress across hydrological and ecological systems. The CEI is the calculated over 81 distinct DS-WS combinations, derived in section 4.3. (from individual DS and WS durations and intensities) across all spatial grids over seven decadal windows spanning across 1951-2019.

Spatial mapping of the decadal CEI values (normalized between 0 and 1; figure S4 (a), Supplementary Material) revealed a sharp decline in whiplash occurrences and spatial coverage during the decade 1981-1990, in contrast to the substantial rise observed in 2011-2019. Therefore, for clearer interpretation and contrast, the further analysis of CEI was stratified into two epochs: 1951-1985 and 1986-2019. This division allowed for a targeted evaluation of pre- and post-1980s dynamics, particularly to examine whether the apparent shift around the 1980s marks a transition point in the evolution of compound extremes.

Building upon the CEI-based assessment, a threshold-based classification was implemented to delineate three whiplash severity categories: Moderate risk (CEI > 60^{th} percentile and ≤ 80^{th} percentile), Severe risk (CEI > 80^{th} percentile and ≤ 95^{th} percentile), Extreme risk (CEI > 95^{th} percentile), for direct comparison of risk levels. While the CEI formulation already accounted for the individual intensities and durations of both DS and WS, to understand the long-term behavioural evolution of whiplash risks at a decadal scale and move beyond isolated events and assess patterns in their temporal recurrence, persistence and cumulative impact, we have further introduced: Frequency (number of decades in which a grid experienced whiplash in a given risk category), Duration (maximum number of consecutive decades during which the grid remained exposed to that category of the whiplash risk), and Intensity (mean normalized CEI over the selected decades for that category, reflecting the mean severity).

https://doi.org/10.5194/egusphere-2025-6498
Preprint. Discussion started: 17 February 2026

When the risk characteristics were compared across the epochs (figure 6(a)), Extreme Whiplash events showed the highest increase in frequency (13 %), followed by Severe (8.7 %), while Moderate Whiplash showed the highest increase in duration (6.3 %) during 1986-2019. Although the intensities across all the risk categories may have plateaued, Extreme Whiplash showed a slight decrease in duration (1.6 %) during 1986-2019. The spatial footprints provided in Supplementary Figure S4(b) corroborate the intensification, revealing a clear expansion in the geographical spread of these events. Figures S4(d) provides an additional resolution by displaying the grid-level distribution of the characteristics of each whiplash category. Majority of grids were concentrated over increased frequency and duration of the moderate-to-severe risk spectrum during 1986-2019. However a comparison with Figure S4(c) (epoch1: 1951-1985) reveals a striking 26.6 % increase in the number of grids experiencing simultaneous high frequency, duration, and intensity, across moderate and extreme whiplash risk category, suggesting a broadening of systemic exposure.

The temporal transitions in overall whiplash risk have been analyzed using CEI (figure 6(d)). While north-west (BSh), and south-east India (CWa) witnessed stable moderate risks throughout 1951-2019, the East coast (Aw), parts of central India (Aw), southern Kerala (Am), and the north-east India (Am) are observing an emerging risk during 1986-2019. Most notably, the entire south-west coast (Am) including Kerala, coastal Karnataka and Maharashtra, and warm temperate North Bengal and parts of the Northeast and northern India (CWb) has sustained a persistently high-risk state since 1951-1985, with no signs of recovery, pointing to chronic exposure. The presence of very few grids showing reducing or no risk in recent decades is alarming and emphasizes the pervasive nature of whiplash intensification across India.

Decadal assessment of climate-yield interactions (figure 6(c)) reveals a distinct transition from technological buffering to climate-induced suppression. While the 1990s exhibited a peak positive anomaly (+173.3 kg/ ha), indicative of technological dominance, the post-2000 era is characterized by persistent negative anomalies (-41.8 and -49.7 kg/ ha for 2000s and 2010s respectively), despite continuous agronomic advancements. This reversal coincides with an expansion in the spatial extent of climate risks; the 2010s recorded the historical maximum area under Extreme risk (2.08 %). Notably, yield deviations exhibited a stronger negative correlation with the area under Severe risk ($r = -0.28$) compared to Extreme risk ($r = -0.06$). This suggests that widespread, moderate-to-severe whiplash stress events compromise national aggregate yields more significantly than intense but spatially localized extremes. The distinct shift to negative yield anomalies in the last two decades evidences a

https://doi.org/10.5194/egusphere-2025-6498
Preprint. Discussion started: 17 February 2026

‘climate penalty’ that has effectively neutralized the marginal gains from recent technological inputs.

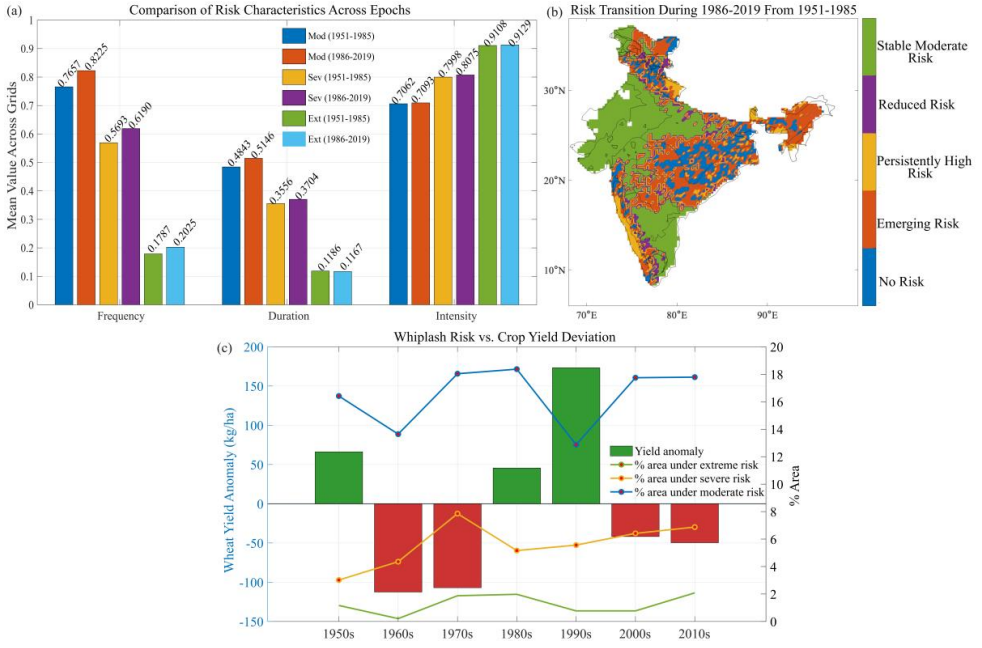

Figure 6: (a) Comparison of normalized characteristics (frequency, duration, and intensity) of Moderate, Severe, and Extreme Whiplash risks between 1951-1985 and 1986-2019; (b) Transition map of overall compound whiplash risk using CEI, comparing the recent epoch 1986-2019 to the baseline epoch 1951-1985; (c) Divergence of wheat yields and whiplash risk (1951-2019), showing decadal detrended yield anomalies (bars) against the temporal evolution of the spatial extent (%) of Moderate, Severe, and Extreme risks, to highlight the increasing impact of whiplash on yield stability.

This persistent and spatially expanding risk has also translated into significant socio-environmental consequences, particularly in regions where high whiplash exposure intersects with vulnerable populations and dynamic land use shifts (figure S5, Supplementary Material). Tropical wet and dry parts of Madhya Pradesh (80.37 %), arid parts of Rajasthan (67.75 %), semi-arid Gujarat (65 %), tropical Kerala (43.5 %), Maharashtra (51.6 %) and Goa (51.85 %) emerged as the most critically exposed states, when compounded with significant land use transitions between 2000 and 2019, including rapid urban expansion, increase in fallow lands, and reduction in plantation cover.

5. Conclusions

https://doi.org/10.5194/egusphere-2025-6498
Preprint. Discussion started: 17 February 2026

This study provides the first pan-India, event-based assessment of the climatology and evolution of individual and compound dry (DS) and wet spells (WS) across India from 1951 to 2019, revealing the emergence of precipitation "whiplash" as a distinct hydroclimatic phenomenon. Unlike previous studies that predominantly examined seasonal or annual drought and flood frequencies, this analysis captures daily-scale transitions and lag-dependent coupling between extremes, allowing for a more mechanistic understanding of abrupt hydroclimatic reversals.

Extreme WS showed broad scale intensification, after a decrease till the 1990s, with a spatial increase of almost 33 % over arid Rajasthan, coastal Karnataka, tropical parts of Kerala and Northeast, while extreme DS exhibited a southward extension from its traditional northwestern core, with an overall spatial increase of 15-40 % over western Rajasthan, central India, and parts of Telangana and Chhattisgarh. This shift indicates a re-distribution of DS dominance from Northwest India, as noted by earlier studies (Mujumdar et al., 2020; Mukherjee et al., 2018), toward more humid and transitional zones. While past studies largely focused on mean monsoon variability and trend asymmetry in rainfall extremes (Verma et al., 2022; Roxy et al., 2017), this study demonstrates a systemic transition towards higher-frequency, higher-intensity precipitation variability, evident through coupled wet-dry dynamics.

A marked post-1980s escalation in both frequency and severity of abrupt whiplash transitions is evident, with spatial footprints expanding into the arid and semi-arid zones of western India, the upper south-west coast and parts of Central India, showing no signs of recovery. Furthermore, the identification of asymmetric whiplash dynamics, increasingly dominated by dry-to-wet transitions, reveals a sharp rise in both intensity (~49 %) and coincidence rates (> 0.8) in several regions, suggesting that dry antecedent conditions amplify subsequent wet responses through soil moisture-precipitation feedbacks. A key methodological advance of this study lies in quantifying the sensitivity of whiplash detection to lag periods, demonstrating that although most transitions occurred abruptly, their decrease with the increase in lag period and almost 50 % increase with longer time windows suggest multi-annual memory and persistence in hydroclimatic system.

Among 81 unique whiplash categories identified, moderately prolonged DS (6-months) followed by a short intense WS, emerged as the most frequent combination, with whiplash frequency peaking (73 % increase) before declining at longer DS durations. This indicates that seasonal-scale dry spells are the most susceptible to abrupt wet reversals. While the "Worst Case" remained concentrated in arid/semi-arid Western India, the "Best Case" and "Flash

https://doi.org/10.5194/egusphere-2025-6498
Preprint. Discussion started: 17 February 2026

Case" expanded into Central and Western zones during the later decades, signalling an emerging eastward redistribution of whiplash risk.

By moving beyond siloed analyses of wet and dry extremes, this study redefines hydroclimatic whiplash as a distinct, emergent compound risk. This further corroborates the increase in extreme whiplash risk frequency by 13 %, with an overall systemic whiplash spatial intensification of 26.6 %. While arid, semi-arid, and tropical wet and dry southeast India emerged as the epicentres of the persistent moderate whiplash stress, the east coast and Central India face rapidly emerging risks, and tropical and temperate regions of south-west coast and northern India respectively, have remained in a persistently high risk state since 1951, showing no signs of recovery, consistent with persistent monsoon variability reported by Roxy et al. (2017) but captured here through a compound lens for the first time. This volatility has already breached agricultural tolerance which collapsed into a post-2000 'climate penalty'.

This study also opens up critical questions for the future. The challenge to provide a physical explanation for many of the observed whiplash patterns remains owing to the complexity of the systems driving individual extremes and the intricate interactions between them. The underlying drivers and mechanisms of whiplash transitions are the focus of ongoing research, which will enable us to disentangle the relative roles of large-scale circulation, local feedbacks, and human-induced changes.

Code and data availability

The data and MATLAB codes used for the whiplash analysis are available at (Bhattacharjee and Dhanya, 2025). The crop yield data is freely obtained from Ministry of Agriculture and Farmers Welfare, Government of India.

Author contributions

Bhattacharjee D.: Writing—original draft, Writing—review and editing, Visualization, Formal Analysis, Investigation, Conceptualization. **Dhanya C.T.:** Writing-—Review and editing, Validation, Supervision, Resources, Formal Analysis, Conceptualization.

Competing Interest

The authors declare that they have no known competing financial interests or personal relationships that could have appeared to influence the work reported in this paper.

https://doi.org/10.5194/egusphere-2025-6498
Preprint. Discussion started: 17 February 2026

References

Anderson, B. J., Muñoz-Castro, E., Tallaksen, L. M., Matano, A., Götte, J., Armitage, R., ... and Brunner, M. I.: What is a drought-to-flood transition? Pitfalls and recommendations for defining consecutive hydrological extreme events. *Hydrology and Earth System Sciences*, *29*(21), 6069-6092, 2025.

Ansari, R., and Grossi, G.: Spatio-temporal evolution of wet–dry event features and their transition across the Upper Jhelum Basin (UJB) in South Asia. *Natural Hazards and Earth System Sciences*, *22*(2), 287-302, 2022.

Alipour, A., Ahmadalipour, A. and Moradkhani, H.: Assessing flash flood hazard and damages in the southeast United States. Journal of Flood Risk Management, 13(2), p.e12605, 2020.

Ayantika, D. C., Krishnan, R., Singh, M., Swapna, P., Sandeep, N., Prajeesh, A. G., and Vellore, R.: Understanding the combined effects of global warming and anthropogenic aerosol forcing on the South Asian monsoon. *Climate Dynamics*, *56*(5), 1643-1662, 2021.

Beck, H. E., Zimmermann, N. E., McVicar, T. R., Vergopolan, N., Berg, A., and Wood, E. F.: Present and future Köppen-Geiger climate classification maps at 1-km resolution. *Scientific data*, *5*(1), 1-12, 2018.

Bhattacharjee, D., and Dhanya, C. T.: Mapping the Rise of Whiplash Risk in India's Hydroclimate (Versio 1.0). Zenodo. https://doi.org/10.5281/zenodo.17810443, 2025.

Bhattacharyya, S., Sreekesh, S., and King, A.: Characteristics of extreme rainfall in different gridded datasets over India during 1983–2015. *Atmospheric Research*, *267*, 105930, 2022.

Borrelli, P., Robinson, D.A., Panagos, P., Lugato, E., Yang, J.E., Alewell, C., Wuepper, D., Montanarella, L. and Ballabio, C.: Land use and climate change impacts on global soil erosion by water (2015-2070). Proceedings of the National Academy of Sciences, 117(36), pp.21994-22001, 2020.

Casson, N.J., Contosta, A.R., Burakowski, E.A., Campbell, J.L., Crandall, M.S., Creed, I.F., Eimers, M.C., Garlick, S., Lutz, D.A., Morison, M.Q. and Morzillo, A.T.: Winter weather whiplash: Impacts of meteorological events misaligned with natural and human systems in seasonally snow-covered regions. Earth's Future, 7(12), pp.1434-1450, 2019.

Christian, J., Christian, K., and Basara, J. B.: Drought and pluvial dipole events within the great plains of the United States. *Journal of Applied Meteorology and Climatology*, *54*(9), 1886–1898, 2015.

https://doi.org/10.5194/egusphere-2025-6498
Preprint. Discussion started: 17 February 2026

637 Coles, S., Bawa, J., Trenner, L., and Dorazio, P.: *An introduction to statistical modeling of*
638 *extreme values* (Vol. 208, p. 208). London: Springer, 2001.
639 Dash, S., and Maity, R.: Revealing alarming changes in spatial coverage of joint hot and wet
640 extremes across India. *Scientific Reports*, *11*(1), 18031, 2021.
641 Diffenbaugh, N. S., Swain, D. L., and Touma, D.: Anthropogenic warming has increased
642 drought risk in California. *Proceedings of the National Academy of Sciences*, *112*(13), 3931–
643 3936, 2015.
644 Dirmeyer, P. A., Schlosser, C. A., and Brubaker, K. L.: Precipitation, recycling, and land
645 memory: An integrated analysis. *Journal of Hydrometeorology*, *10*(1), 278-288, 2009.
646 Donges, J. F., Schleussner, C. F., Siegmund, J. F., and Donner, R. V.: Coincidence analysis for
647 quantifying statistical interrelationships between event time series. *arXiv preprint*
648 *arXiv:1508.03534,* 2015.
649 Donges, J., Schleussner, C.-F., Siegmund, J., and Donner, R.: Event coincidence analysis for
650 quantifying statistical interrelationships between event time series. *The European Physical*
651 *Journal Special Topics*, *225*(3), 471–487, 2016.
652 Getis, A., and Ord, J. K.: The analysis of spatial association by use of distance
653 statistics. *Geographical analysis*, *24*(3), 189-206, 1992.
654 Götte, J., and Brunner, M. I.: Hydrological drought-to-flood transitions across different
655 hydroclimates in the United States. *Water Resources Research*, *60*(7), e2023WR036504, 2024.
656 Goswami, B. N., Venugopal, V., Sengupta, D., Madhusoodanan, M. S., and Xavier, P. K.:
657 Increasing trend of extreme rain events over India in a warming
658 environment. *Science*, *314*(5804), 1442-1445, 2006.
659 Guttman, N. B.: Comparing the palmer drought index and the standardized precipitation index
660 1. *JAWRA Journal of the American Water Resources Association*, *34*(1), 113-121, 1998.
661 He, X., Wada, Y., Wanders, N., and Sheffield, J.: Intensification of hydrological drought in
662 California by human water management. *Geophysical Research Letters*, *44*, 1777–1785.
663 https://doi.org/10.1002/2016GL071665, 2017.
664 He, X. and Sheffield, J.: Lagged compound occurrence of droughts and pluvials globally over
665 the past seven decades. Geophysical Research Letters, 47(14), p.e2020GL087924, 2020.
666 Henn, B., Musselman, K. N., Lestak, L., Ralph, F. M., and Molotch, N. P.: Extreme runoff
667 generation from atmospheric river driven snowmelt during the 2017 Oroville Dam spillways
668 incident. *Geophysical Research Letters*, *47*(14), e2020GL088189, 2020.
669 IPCC: Climate change 2021: The physical science basis. Contribution of working group I to
670 the sixth assessment report of the intergovernmental panel on climate change. V. Masson-

https://doi.org/10.5194/egusphere-2025-6498
Preprint. Discussion started: 17 February 2026

671 Delmotte, P. Zhai, A. Pirani, S. L. Connors, C. Péan, and S. Berger Editors
672 (Cambridge: Cambridge University Press), 2021.
673 Johnston, E.: *Impact of Climate Variability on Landslide Hazard in the Western United States*.
674 Stanford University, 2024.
675 Johnston, E.C., Davenport, F.V., Wang, L., Caers, J.K., Muthukrishnan, S., Burke, M. and
676 Diffenbaugh, N.S.: Quantifying the effect of precipitation on landslide hazard in urbanized and
677 non-urbanized areas. Geophysical Research Letters, 48(16), p.e2021GL094038, 2021.
678 Katzenberger, A., Schewe, J., Pongratz, J., and Levermann, A.: Robust increase of Indian
679 monsoon rainfall and its variability under future warming in CMIP-6 models. *Earth System*
680 *Dynamics Discussions*, *2020*, 1-30, 2020.
681 Krishna, U. V. M., Das, S. K., Sulochana, E. G., Utsav, B., Deshpande, S. M., and Pandithurai,
682 G.: Statistical characteristics of raindrop size distribution over Western Ghats of India: wet
683 versus dry spells of Indian Summer Monsoon. *Atmospheric Chemistry and Physics*
684 *Discussions*, *2020*, 1-65, 2020.
685 Krishnan, R., Gnanaseelan, C., Sanjay, J., Swapna, P., Dhara, C., Sabin, T.P., Jadhav, J.,
686 Sandeep, N., Choudhury, A.D., Singh, M. and Mujumdar, M.: Introduction to climate change
687 over the Indian region. Assessment of climate change over the indian region: a report of the
688 ministry of earth sciences (MoES), Government of India, pp.1-20, 2020.
689 Kumar, K. N., Rajeevan, M., Pai, D. S., Srivastava, A. K., and Preethi, B.: On the observed
690 variability of monsoon droughts over India. *Weather and Climate Extremes*, *1*, 42-50, 2013.
691 Kumar, R. and Mishra, V.: Increase in population exposure due to dry and wet extremes in
692 India under a warming climate. Earth's Future, 8(12), p.e2020EF001731, 2020.
693 Köppen, W.: The heat zones of the earth, viewed according to the duration of the hot, temperate
694 and cold periods and the effect of heat on the organic world. Meteorological Journal , 1 (21),
695 pp.5-226, 1884.
696 Koskinas, A., Tegos, A., Tsira, P., Dimitriadis, P., Iliopoulou, T., Papanicolaou, P., ... and
697 Williamson, T.: Insights into the Oroville dam 2017 spillway incident. *Geosciences*, *9*(1), 37,
698 2019.
699 Koster, R. D., Mahanama, S. P. P., Yamada, T. J., Balsamo, G., Berg, A. A., Boisserie, M., ...
700 and Wood, E. F.: Contribution of land surface initialization to subseasonal forecast skill: First
701 results from a multi-model experiment. *Geophysical Research Letters*, *37*(2), 2010.
702 Laimighofer, J., and Laaha, G.: How standard are standardized drought indices? Uncertainty
703 components for the SPI and SPEI case. *Journal of Hydrology*, *613*, 128385, 2022.

https://doi.org/10.5194/egusphere-2025-6498
Preprint. Discussion started: 17 February 2026

Lin, L., Wang, Z., Xu, Y., Zhang, X., Zhang, H. and Dong, W.: Additional intensification of seasonal heat and flooding extreme over China in a 2 C warmer world compared to 1.5 C. Earth's Future, 6(7), pp.968-978, 2018.

Liu, W., Zhang, Q., Li, C., Xu, L., and Xiao, W.: The influence of soil moisture on convective activity: a review. *Theoretical and Applied Climatology*, *149*(1), 221-232, 2022.

Madakumbura, G.D., Thackeray, C.W., Norris, J., Goldenson, N. and Hall, A.: Anthropogenic influence on extreme precipitation over global land areas seen in multiple observational datasets. *Nature Communications*, 12(1), p.3944, 2021.

Masson-Delmotte, V., Zhai, P., Pirani, A., Connors, S. L., Péan, C., Berger, S., ... and Zhou, B.: Climate change 2021: the physical science basis. *Contribution of working group I to the sixth assessment report of the intergovernmental panel on climate change*, *2*(1), 2391, 2021.

Miralles, D. G., Gentine, P., Seneviratne, S. I., and Teuling, A. J.: Land–atmospheric feedbacks during droughts and heatwaves: state of the science and current challenges. *Annals of the New York Academy of Sciences*, *1436*(1), 19-35, 2019.

Mishra, V., Nanditha, J. S., Dangar, S., Chuphal, D. S., and Vegad, U.: Drivers, changes, and impacts of hydrological extremes in India: A review. *Wiley Interdisciplinary Reviews: Water*, *11*(5), e1742, 2024.

Mukherjee, S., Aadhar, S., Stone, D., and Mishra, V.: Increase in extreme precipitation events under anthropogenic warming in India. *Weather and climate extremes*, *20*, 45-53, 2018.

Mukherjee, S., Mishra, A., and Trenberth, K. E.: Climate change and drought: a perspective on drought indices. *Current climate change reports*, *4*, 145-163, 2018.

Mujumdar, M., Bhaskar, P., Ramarao, M. V. S., Uppara, U., Goswami, M., Borgaonkar, H., ... and Niyogi, D.: Droughts and floods. In *Assessment of climate change over the Indian region: a report of the Ministry of Earth Sciences (MoES), Government of India* (pp. 117-141). Singapore: Springer Singapore, 2020.

Otkin, J. A., Anderson, M. C., Hain, C., Mladenova, I. E., Basara, J. B., and Svoboda, M.: Examining rapid onset drought development using the thermal infrared–based evaporative stress index. *Journal of Hydrometeorology*, *14*(4), 1057-1074, 2013.

Pai, D., Sridhar, L., Rejeevan, M., Sreejith, O., Satbhai, N., and Mukhopadhyay, B.: Development of a new high spatial resolution (0.25° × 0.25°) long period (1901–2010) daily gridded rainfall data set over India and its comparison with existing data sets over the region. . *Mausam, 65*(1), 1-18, 2014.

https://doi.org/10.5194/egusphere-2025-6498
Preprint. Discussion started: 17 February 2026

Pal, L., and Ojha, C. S. P.: Characteristics of soil moisture droughts in ganga river basin during 1948–2015. In *The Ganga River Basin: A Hydrometeorological Approach* (pp. 291-308). Cham: Springer International Publishing, 2021.

Peel, M. C., Finlayson, B. L., and McMahon, T. A.: Updated world map of the Köppen-Geiger climate classification. *Hydrology and earth system sciences*, *11*(5), 1633-1644, 2007.

Pendergrass, A. G., Knutti, R., Lehner, F., Deser, C., and Sanderson, B. M.: Precipitation variability increases in a warmer climate. *Scientific reports*, *7*(1), 17966, 2017.

Rehana, S., Yeleswarapu, P., Basha, G., and Munoz-Arriola, F.: Precipitation and temperature extremes and association with large-scale climate indices: An observational evidence over India. *Journal of Earth System Science*, *131*(3), 170, 2022.

Roxy, M. K., Ghosh, S., Pathak, A., Athulya, R., Mujumdar, M., Murtugudde, R., ... and Rajeevan, M.: A threefold rise in widespread extreme rain events over central India. *Nature communications*, *8*(1), 708, 2017.

Salvadori, G., Michele, C. D., Kottegoda, N. T., and Rosso, R.: *Extremes in nature: an approach using copulas*. Dordrecht: Springer Netherlands, 2007.

Scasta, J. D., Weir, J. R., and Stambaugh, M. C.: Droughts and wildfires in western US rangelands. *Rangelands*, *38*(4), 197-203, 2016.

Seneviratne, S. I., Corti, T., Davin, E. L., Hirschi, M., Jaeger, E. B., Lehner, I., ... and Teuling, A. J.: Investigating soil moisture–climate interactions in a changing climate: A review. *Earth-Science Reviews*, *99*(3-4), 125-161, 2010.

Siegmund, J. F., Siegmund, N., and Donner, R. V.: CoinCalc—A new R package for quantifying simultaneities of event series. *Computers and Geosciences*, *98*, 64–72, 2017.

Singh, G.R., Dhanya, C.T. and Chakravorty, A., 2021. A robust drought index accounting changing precipitation characteristic. Water Resources Research, 57(7), p.e2020WR029496.

Singh, N., and Ranade, A.: The wet and dry spells across India during 1951–2007. *Journal of Hydrometeorology*, *11*(1), 26-45, 2010.

Straus, D. M.: Preferred intra-seasonal circulation patterns of the Indian summer monsoon and active-break cycles: a new view of the active-break cycle. *Climate Dynamics*, *59*(5), 1415-1434, 2022.

Swain, D. L., Langenbrunner, B., Neelin, J. D., and Hall, A.: Increasing precipitation volatility in twenty-first-century California. *Nature Climate Change*, *8*(5), 427-433, 2018.

Swain, D.L.: A shorter, sharper rainy season amplifies California wildfire risk. Geophysical Research Letters, 48(5), p.e2021GL092843, 2021.

https://doi.org/10.5194/egusphere-2025-6498
Preprint. Discussion started: 17 February 2026

769 Tan, X., Wu, X., Huang, Z., Fu, J., Tan, X., Deng, S., ... and Liu, B.: Increasing global
770 precipitation whiplash due to anthropogenic greenhouse gas emissions. *Nature*
771 *Communications*, *14*(1), 2796, 2023.
772 Tandel, D., Verma, S., Kumar, K., and Verma, M. K.: Impact assessment of wet and dry spell
773 on agriculture productivity of Chhattisgarh, India. *Journal of Environmental Informatics*
774 *Letters*, *10*(1), 10-22, 2023.
775 Trenberth, K. E., Dai, A., Rasmussen, R. M., and Parsons, D. B.: The changing character of
776 precipitation. *Bulletin of the American Meteorological Society*, *84*(9), 1205–1218, 2003.
777 Verma, S., Bhatla, R., Shahi, N. K., and Mall, R. K.: Regional modulating behavior of Indian
778 summer monsoon rainfall in context of spatio-temporal variation of drought and flood
779 events. *Atmospheric Research*, *274*, 106201, 2022.
780 Vinnarasi, R. and Dhanya, C.T.: Changing characteristics of extreme wet and dry spells of
781 Indian monsoon rainfall. Journal of Geophysical Research: Atmospheres, 121(5), pp.2146-
782 2160, 2016.
783 Vicente-Serrano, S. M., Beguería, S., and López-Moreno, J. I.: A multi-scalar drought index
784 sensitive to global warming: the standardized precipitation evapotranspiration index. *Journal*
785 *of climate*, *23*(7), 1696-1718, 2010.
786 Vose, R. S., Applequist, S., Bourassa, M. A., Pryor, S. C., Barthelmie, R. J., Blanton, B., ...
787 and Young, R. S.: Monitoring and understanding changes in extremes: Extratropical storms,
788 winds, and waves. *Bulletin of the American Meteorological Society*, *95*(3), 377-386, 2014.
789 Walters, B. B.: An event-based methodology for climate change and human–environment
790 research. *Geografisk Tidsskrift-Danish Journal of Geography*, *112*(2), 135-143, 2012.
791 Weesie, R. V., Rohse, M., Van Loon, A. F., Koehler, J., Barendrecht, M. H., and Mwangi, M.:
792 Floods after drought: storytelling with agro-pastoralists in a Kenyan dryland. *Frontiers in*
793 *Water*, *7*, 1524554, 2025.
794 Wilhite, D. A., and Glantz, M. H.: Understanding: the drought phenomenon: the role of
795 definitions. *Water international*, *10*(3), 111-120, 1985.
796 Zhang, X., Wang, C., Chen, X., Dong, J., Hu, M., and Liu, S.: Insights into the cause of the
797 Oroville dam spillway failure, 2017, California. *Environmental Science and Pollution*
798 *Research*, *31*(14), 21356-21369, 2024.
799 Zhou, X., and Geerts, B.: The influence of soil moisture on the planetary boundary layer and
800 on cumulus convection over an isolated mountain. Part I: Observations. *Monthly weather*
801 *review*, *141*(3), 1061-1078, 2013.

https://doi.org/10.5194/egusphere-2025-6498
Preprint. Discussion started: 17 February 2026

802 Zscheischler, J., Westra, S., Van Den Hurk, B. J., Seneviratne, S. I., Ward, P. J., Pitman, A., ...
803 and Zhang, X.: Future climate risk from compound events. *Nature climate change*, *8*(6), 469-
804 477, 2018.